

Perspective Article

Polymeric nanoassembly of imine functionalized magnetite for loading copper salts to catalyze Henry and A³-coupling reactionsPrakash B. Rathod^{a,b,c}, K.S. Ajish Kumar^d, Anjali A. Athawale^a, Ashok K. Pandey^{b,e,*}^a Department of Chemistry, Savitribai Phule Pune University, Pune 411007, India^b Radiochemistry Division, Bhabha Atomic Research Centre, Trombay, Mumbai 400085, India^c Department of Chemistry, Shree Sadguru Saibaba Science college, Ashti 442707, Maharashtra, India^d Bio-Organic Division, Bhabha Atomic Research Centre, Trombay, Mumbai 400085, India^e Homi Bhabha National Institute, Anushaktinagar, Mumbai 400094, India

ARTICLE INFO

Keywords:

Magnetite
Copper(II)-imine complex
Catalysis
Henry reaction
A³-couplings

ABSTRACT

Poly(ethylenimine) was grafted on the magnetite (Fe₃O₄) nanoparticles, and subsequently reacted with different aldehydes to form the imine functionalities (Fe₃O₄-Imine NPs). Thus formed Fe₃O₄-Imine NPs could host copper salts generally used as the homogeneous catalyst in organic reactions with the stability prerequisite for the recycling. The expected chemical structures of Fe₃O₄-Imine NPs were ascertained by the FTIR and CHNS analyses. The physical structure of Fe₃O₄-Imine NPs was found to be corn-like assemblies from the images obtained by FESEM and HRTEM. The Fe₃O₄-Imine NPs assemblies possessed the superparamagnetic properties which made possible to withdraw these particles from the reaction solution efficiently. The copper salt loading capacity of the Fe₃O₄-Imine was lower than that of the Fe₃O₄-PEI, but the water content in the Fe₃O₄-Imine was higher (10 wt%) than that of the Fe₃O₄-PEI (2.5 wt%). Among different aldehydes and copper salts used, the Fe₃O₄-Imine formed by benzaldehyde and loaded with copper acetate salt exhibited better catalytic activity in the Henry reactions using water as the solvent. Also, the Fe₃O₄-Imine showed better catalytic activity than that obtained using the Fe₃O₄-PEI in both Henry reactions and A³-coupling of aldehyde, pyrrolidine, and phenyl acetylene reactants. The several representative examples of these coupling reactions were studied to understand the different parameters affecting the catalytic efficacy of copper acetate loaded Fe₃O₄-Imine.

1. Introduction

Green chemical processes require a design of the new multifunctional nanocatalysts for the tandem reactions in one pot [1]. The extensive studies are being carried out to explore the functional nanomaterial as the catalysts due to their high surface area which makes them intermediate between homogeneous and heterogeneous catalysts [2]. The functionalized polymers could be used not only for anchoring of the desired catalysts on the host matrix but also forming the functional groups that can bind with the known homogeneous catalysts [3–6]. The magnetic nanoparticles (MNPs) have been attracting special attention as the heterogeneous catalyst supports because of their higher dispersion in the reaction solution and also the superparamagnetic behavior which enable their easy withdrawal from the reaction media under the magnetic field [7–9]. Among different MNPs, the iron oxide based magnetic nanoparticles (MNPs) offers several advantages including anchoring

homogeneous catalysts without involving complicated synthetic chemistry [10–12]. It has been reported that the bare magnetite MNPs could be used directly for catalyzing the selected organic reactions [12–14]. However, the functionalization of MNPs is a key factor to make a stable and selective catalyst. Therefore, the iron based MNPs have been studied extensively for the functionalization to generate the desired catalytic sites [15–23]. The recent uses of the polymer grafted nanoparticles show great potential in a variety of applications, including advanced polymer nanocomposite fabrication, drug delivery, imaging, catalysis and lubrication [24–26].

The copper is one of the prime elements in catalyzing the organic transformations. This is because of its ability to form numbers of complexes with the reagents and also due to their higher abundance which makes it more cost effective and more sustainable than the precious transition metal/noble metal based catalysts [27]. The general examples of copper catalyzed reactions are the Click reactions, asymmetric

* Corresponding author at: Radiochemistry Division, Bhabha Atomic Research Centre, Trombay, Mumbai 400085, India.

E-mail address: ashokk@barc.gov.in (A.K. Pandey).<https://doi.org/10.1016/j.reactfunctpolym.2021.104868>

Received 15 November 2020; Received in revised form 19 February 2021; Accepted 22 February 2021

Available online 26 February 2021

1381-5148/© 2021 Elsevier B.V. All rights reserved.

acetylide additions to carbonyl groups, radical alkylations, asymmetric conjugate additions etc. [28–32]. Henry reactions, also known as the nitroaldol reactions, are important in synthetic organic chemistry as these reactions are used for the coupling of a nucleophilic nitroalkane with an electrophilic aldehyde or ketone to produce a synthetically useful β -nitro alcohol [33–37]. The examples of variations of the nitroaldol reactions are nitronate condensations, Retro-Henry reaction, intramolecular Henry reaction etc. [38]. The base-catalyzed Henry reactions have the problems of various competitive side reactions such as Nef-type reactions. Also, the base-catalyzed elimination of water can lead to the formation of readily polymerizable nitro-olefin. To address these problems, several homogeneous and heterogeneous catalysts, including magnetic nanoparticles supported catalysts, have been developed for the selective Henry reactions [39–47]. Biradar et al. have reported a fixed bed reactor packed with the primary or secondary amine-functionalized mesoporous silica (MCM-41) for performing continuous Henry reaction [48]. It is reported in the literature that the copper complexes are efficient in catalyzing this class of reactions [42–47]. The copper has been immobilized on the amine rich magnetic glycocyanine-modified chitosan which was found to have good catalytic activity in the A^3 -coupling reactions of aldehydes, secondary amines and phenyl acetylene for the propargylamines preparation [49]. The poly(ethylenimine) is known to have a higher affinity towards Cu(II) ions [50]. However, the catalytic efficiency of the Cu(II)-loaded poly(ethylenimine) coated magnetite has not been found to be higher for Henry reaction in water [50]. The primary amine groups on poly(ethylenimine) could be converted to imines with aldehydes, which may be more hydrophilic and form a stable complex with copper salts [51]. Thus, the hydrophilic copper salts loaded imine polymeric assemble may exhibit better catalytic activity in the organic reactions in water due to their better compatibility.

In the present work, the different imine-functionalized nanoassemblies of the magnetite particles have been developed to host Cu(II) salts generally employed for catalyzing the several organic reactions. The objective of the present work is to study the catalytic efficiency of a copper salt complexed by an imine functional group anchored on a polymer coating of magnetite NP for the Henry and A^3 coupling reactions. The magnetite NPs (Fe_3O_4) have been subjected to a series of steps to anchor poly(ethylenimine) (PEI) (Fe_3O_4 -PEI), which has been subsequently converted to the imine functionality (Fe_3O_4 -Imine) by reacting with different aldehydes. Thus formed Fe_3O_4 -Imine NPs have been loaded with different copper salts such as copper acetate, copper chloride and copper bromide. The Fe_3O_4 -Imine polymeric nanostructures have been characterized by the CHNS elemental analysis, field emission scanning electron microscopy (FESEM), high resolution transmission electron microscopy (HRTEM), Fourier transform infrared spectroscopy (FTIR), thermo-gravimetric analysis (TGA), and vibrating sample magnetometry (VSM). The catalytic activities of Fe_3O_4 -Imine-Cu(II) polymeric nanoassemblies have been studied for the selected examples of the Henry and A^3 -coupling reactions.

2. Experimental

The details of reagents obtained commercially/prepared in the laboratory are given in Supplementary Material (Appendix A). The formation Fe_3O_4 -PEI was carried out using a similar synthetic protocol described in our earlier publication [50], and discussed here briefly. The Fe_3O_4 -Imine-Cu(II) catalyst was formed by suspending 1 g of Fe_3O_4 MNPs in 200 mL ethanol using sonicator, and added 100 mL of water + 3 mL ammonia solution. This solution mixture was again homogenized with a sonicator and 2 mL of (3-aminopropyl)triethoxy silane (APTES) was added. Finally, this solution was kept for overnight stirring. After overnight stirring, the APTES was coated on Fe_3O_4 which were taken out using an external magnet, washed thoroughly with ethanol and water, and dried in the air after washing. For anchoring PEI, 1 g of APTES coated Fe_3O_4 MNPs were dispersed in 200 mL of DMF having 2 g of poly

(vinylbenzyl chloride) (PVBCl) and kept for a reaction for 12 h. Thus formed PVBCl reacted particles (Fe_3O_4 -PVBCl) were removed using an external magnet and washed several times with DMF/ethanol. In the final step of preparation, the Fe_3O_4 -PVBCl particles were reacted with an excess of PEI dissolved in ethanol at room temperature for 12 h with continuous stirring, and washed thoroughly to obtain cleaned and dried Fe_3O_4 -PEI particles.

In a subsequent chemical modification, the amine functionality of Fe_3O_4 -PEI MNPs converted to imine by reacting with a different aldehyde such as benzaldehyde, sugar aldehyde, (+) camphor, camphor sulphonic acid, 1-tert-butyl-4-methylenecyclohexane, and flavanone in DMF at 60 °C under nitrogen atmosphere. The Fe_3O_4 -Imine MNPs are not very stable. To avoid the backward reaction, the Fe_3O_4 -Imine MNPs were washed with dried acetone and dichloromethane and then suspended instantaneously in the solution containing copper salts in dry acetone. Thus formed catalyst Fe_3O_4 -Imine MNPs were characterized by CHNS analysis, VSM, FESEM, HRTEM, and FTIR.

The NMR spectra were recorded by using Varian, 500 MHz, Inc., USA and the sample was prepared by dissolving 5 mg of product sample in $CDCl_3$ and transferred into NMR tube. The LC-MS spectrometry was carried out by using model number 410 Prostar Binary LC with 500 MS IT PDA Detectors supplied by Varian, Inc. USA. The nitrogen analyses were done at Sophisticated Analytical Instrument Facility (SAIF), IIT-Bombay, Mumbai, India. Scanning Electron Microscopic imaging of Fe_3O_4 particles was also carried out at SAIF using field emission gun scanning electron microscopy (FESEM) (model JSM-7600F). Thermo-gravimetric analysis (TGA) was carried out using STARe system METTLER TOLEDO instrument. For this analysis, the known weight of the sample was taken in an alumina holder and thermo-grams was obtained with heating rate of 10 °C min^{-1} from 30 °C to 900 °C, under dynamic condition and in air atmosphere (50 mL min^{-1}).

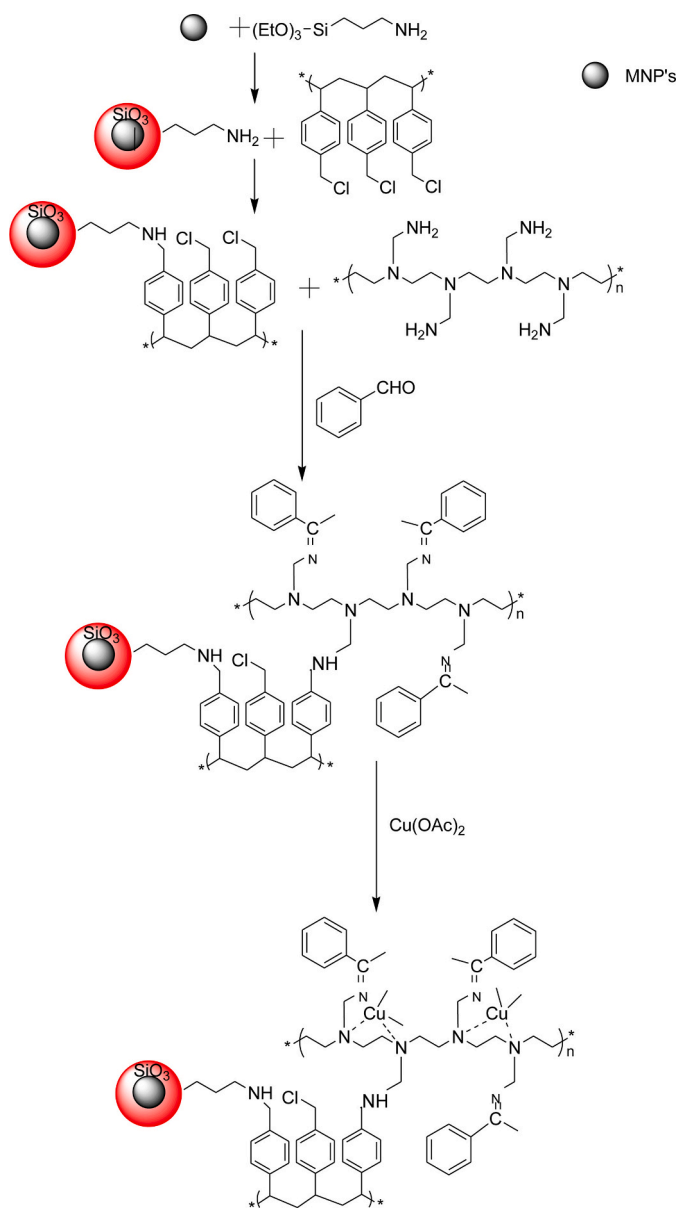
The catalytic activity of the Fe_3O_4 -Imine-Cu(II) was studied in the Henry and A^3 multicomponent couplings reactions. The completion of the reaction was monitored by using TLC. After completion of a reaction, the solution was decanted and the Fe_3O_4 -Imine-Cu(II) catalyst was recovered by using an external magnet and wash with methanol or ethanol. The collected catalyst dried at 50 °C in an oven under vacuum for further use. The decanted solution was concentrated by using rotavapor, treated with silica, and purified by using the column chromatography. The products were analyzed by NMR, IR and HRMS as given in Supplementary Material (Appendix A).

3. Results and discussion

3.1. Grafting of PEI on Fe_3O_4 and conversion to imine

The commercially obtained Fe_3O_4 NPs (12 ± 3 nm size) were coated with (3-aminopropyl)triethoxy silane (APTES) in ethanol and was then reacted with poly(vinylbenzylchloride) (PVBCl) in DMF to form the covalently linked polymer shell on Fe_3O_4 NPs as illustrated in Scheme 1, which is similar to synthetic procedure described in our earlier work [50]. The PVBCl coated Fe_3O_4 NPs were again reacted with low molecular weight poly(ethylenimine) (PEI) ($M_w = 1300$) to form covalent links with the residual benzyl chloride units of PVBCl by replacing covalently bonded chlorine atom as shown in Scheme 1.

Thus formed Fe_3O_4 -PEI NPs possessed higher concentration of the amine sites. The amine groups on Fe_3O_4 -PEI NPs then converted to imine by reacting with different aldehydes in dry DMF solvent at 60 °C under nitrogen atmosphere. The prepared Fe_3O_4 -Imine NPs were loaded with the copper salts in dry solvent acetone. It was observed that the Cu(II) loadings made the anchored imine functionalities on Fe_3O_4 -Imine NPs stable and prevented the imine degeneration due to hydrolysis. The different aldehyde functionality such as benzaldehyde (1a), sugar aldehyde (2a), (+) camphor (3a), camphor sulphonic acid (4a), 1-tert-butyl-4-methylenecyclohexane (5a), and flavanone (6a) were used for the imine formation with Fe_3O_4 -PEI as shown in Scheme 2. The primary



Scheme 1. Illustration of the chemical steps involved in the formation of $\text{Fe}_3\text{O}_4\text{@Imine-Cu(II)}$ catalyst using benzaldehyde (**1a**).

objective of using different aldehyde was to provide rigidity to a copper complex formed on the $\text{Fe}_3\text{O}_4\text{-Imine}$ and also create the different local environment around Cu(II) .

3.2. Characterizations of $\text{Fe}_3\text{O}_4\text{-Imine}$ catalysts

The formations of functional groups in different chemical steps shown in **Scheme 1** were monitored by the elemental analyses and FTIR spectroscopy. As can be seen from Table S1 (Appendix A), the nitrogen (0.39 wt%) and carbon (1.65 wt%) contents confirmed the coating of APTES on Fe_3O_4 NPs. As expected, the carbon content increased to 3.92 wt% and nitrogen content decreased slightly (0.36 wt%) on reacting APTES coated Fe_3O_4 NPs with PVBCL. Finally, the nitrogen content increased to 0.46 wt% on reacting PVBCL coated NPs with PEI indicating the formation of $\text{Fe}_3\text{O}_4\text{-PEI}$. The presence of expected functional groups in each step shown in **Scheme 1** was also confirmed by taking FTIR spectra as shown in Fig. S1 (Appendix A). The FTIR spectrum showed the vibration bands of Fe-O ($550\text{--}570\text{ cm}^{-1}$), Si-O ($1030\text{--}1080\text{ cm}^{-1}$), Si-O-Si ($940\text{--}980\text{ cm}^{-1}$), C=N ($1610\text{--}1660\text{ cm}^{-1}$), C=C

(aromatic, $1250\text{--}1370\text{ cm}^{-1}$), N-H ($3280\text{--}3300\text{ cm}^{-1}$), and -CH_2 (1470 cm^{-1}) confirming the final chemical structure of $\text{Fe}_3\text{O}_4\text{-imine}$ NPs depicted in **Scheme 1**.

The Cu(II) loadings on the $\text{Fe}_3\text{O}_4\text{-Imine}$ NPs formed by using different aldehydes were estimated by energy dispersive X-ray fluorescence analyses by EDS attached to FESEM. It is seen from data given in Table S2 (Appendix A) that the Cu(II) loading was an order of $\approx 1.2\text{ wt\%}$ in all the samples of $\text{Fe}_3\text{O}_4\text{-Imine}$ NPs irrespective of their imine functional groups. However, the Cu(II) loading capacity of $\text{Fe}_3\text{O}_4\text{-PEI}$ reported in our earlier work was higher ($\approx 2.6\text{ wt\%}$) under similar conditions [50]. A similar trend was reported elsewhere wherein Cu loading was found to be reduced after the conversion of a primary amine in PEI to the imine functional groups [51]. Thermogravimetric analysis showed 4-steps thermal degradation of the $\text{Fe}_3\text{O}_4\text{-Imine-Cu(II)}$ (Structure **1a**) NPs with total weight loss of $\sim 18\text{ wt\%}$, see Fig. S2 (Appendix A). The weight loss of 10% in first step of the thermogram of $\text{Fe}_3\text{O}_4\text{-Imine-Cu(II)}$ could be attributed to the loss of free water as bound water would be expected to be released at higher temperature (up to $200\text{ }^\circ\text{C}$). Under similar conditions, 2.5% weight loss from the $\text{Fe}_3\text{O}_4\text{-PEI-Cu(II)}$ was observed [50]. This suggested that the water content in $\text{Fe}_3\text{O}_4\text{-Imine-Cu(II)}$ was higher than that in $\text{Fe}_3\text{O}_4\text{-PEI-Cu(II)}$. The remaining 8 wt% weight loss from the $\text{Fe}_3\text{O}_4\text{-Imine-Cu(II)}$ corresponded to the amount of materials anchored on Fe_3O_4 NPs during coatings and subsequent chemical modifications to form the imine functionalities. This is a significant amount of loading of the material on Fe_3O_4 , and was expected to affect the superparamagnetic properties of Fe_3O_4 NPs adversely. The degradation of superparamagnetic properties of $\text{Fe}_3\text{O}_4\text{-Imine}$ nanoassembly with respect to pristine Fe_3O_4 NPs was studied by vibrating sample magnetometer (VSM). It was observed that the saturation magnetization of $\text{Fe}_3\text{O}_4\text{-Imine}$ was drastically decreased with respect to Fe_3O_4 . However, the superparamagnetic properties were retained i.e. no remanence and coercivity. It is seen from Fig. S3 (Appendix A) that the saturation magnetization was decreased systematically in each step of the formation from Fe_3O_4 to $\text{Fe}_3\text{O}_4\text{-Imine-Cu(II)}$. The $\text{Fe}_3\text{O}_4\text{-Imine-Cu(II)}$ NPs having 4.5 emu g^{-1} saturation magnetization could be retrieved easily using the external magnetic field.

3.3. Morphology of $\text{Fe}_3\text{O}_4\text{-Imine}$ polymeric nanoassemblies

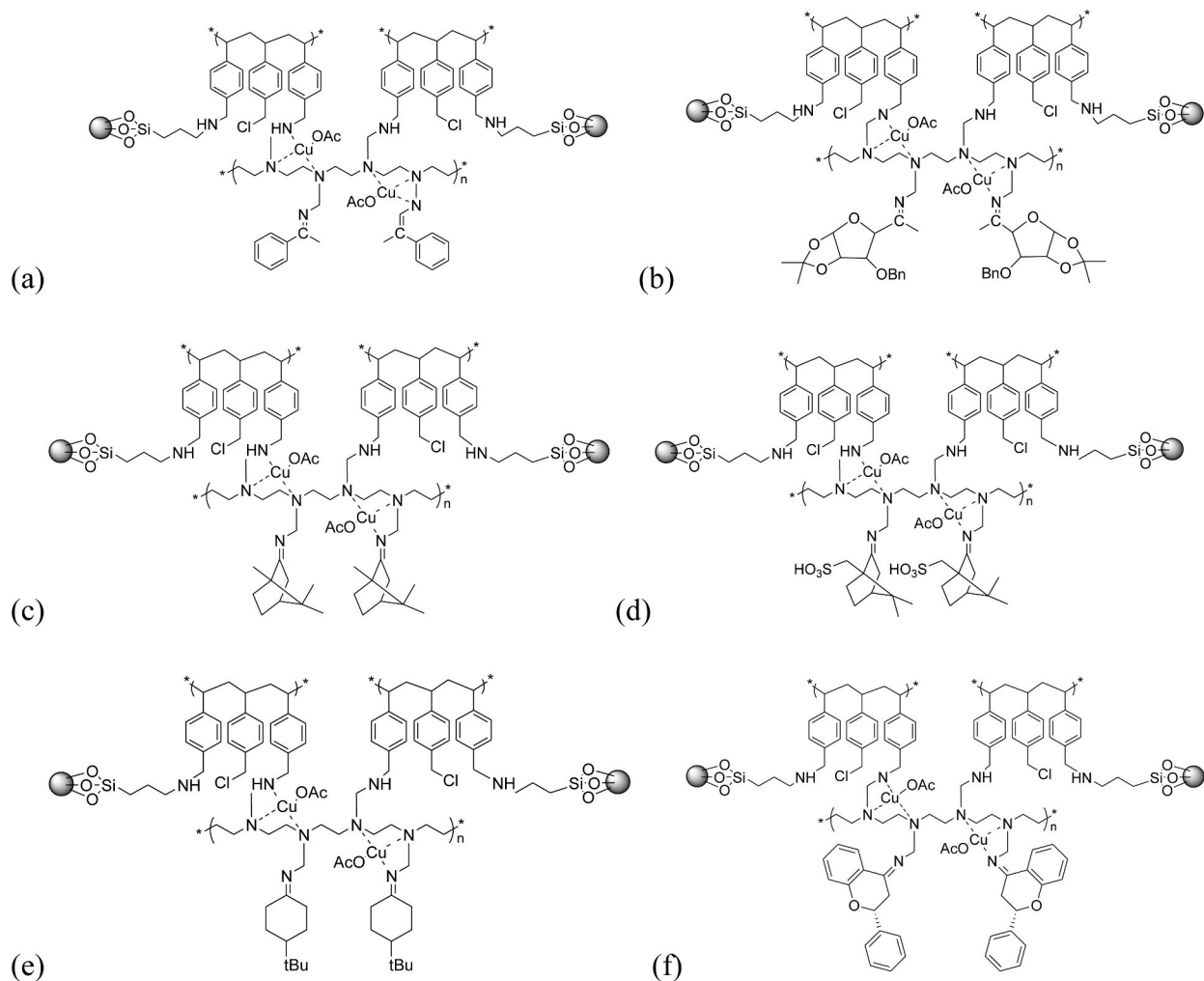
The morphology of the functionalized NPs was studied by FESEM. The representative FESEM images shown in Fig. 1a suggested that the $\text{Fe}_3\text{O}_4\text{-PEI}$ NPs had spherical shapes with overlapping coatings. HRTEM image given in Fig. 1b also showed that the coatings on $\text{Fe}_3\text{O}_4\text{-PEI}$ NPs were polymeric gel-like shell that encapsulated Fe_3O_4 NPs.

It was observed from the representative FESEM images given in Fig. 2 that the $\text{Fe}_3\text{O}_4\text{-PEI}$ NPs aggregated to form the corn-like polymeric assembly with varying length during reaction with an aldehyde. The assembling of NPs in a long corn-like structure was related to reaction conditions (DMF at $60\text{ }^\circ\text{C}$ under nitrogen atmosphere) used for the formation of imine which led to the fractal like growth. The representative HRTEM images $\text{Fe}_3\text{O}_4\text{-Imine}$ NPs are shown in Fig. 3. It is seen from HRTEM images that it was the coated shell that formed the corn-like nanoassemblies having Fe_3O_4 NPs embedded in the interior matrices.

The illustration of morphological changes during different steps involved in the formation of corn shaped $\text{Fe}_3\text{O}_4\text{-Imine}$ assembly are depicted in **Scheme 3**. The stability of these corn assemblies was attributed to the interparticle crosslinking between free amine and residual benzyl chloride units of PVBCL as well as overlapping of the polymer shells of two adjacent particles.

3.4. Henry reaction using $\text{Fe}_3\text{O}_4\text{-Imine-Cu(II)}$ catalyst

The $\text{Fe}_3\text{O}_4\text{-Imine-Cu(II)}$ NPs were studied for their catalytic efficiencies in the Henry type nitroaldol formation reactions. To optimize the reaction conditions, a model reaction of 3-nitrobenzaldehyde with nitromethane shown in **Scheme 4** was conducted under different



Scheme 2. Different imine functional groups formed by reacting Fe_3O_4 -PEI with: (a) benzaldehyde (**1a**), (b) sugar acrylamide (**2a**), (c) (+) camphor (**3a**), (d) (+) camphor sulphonic acid (**4a**), (e) 1-tert-butyl-4-methylenecyclohexane (**5a**), and (f) flavanone (**6a**).

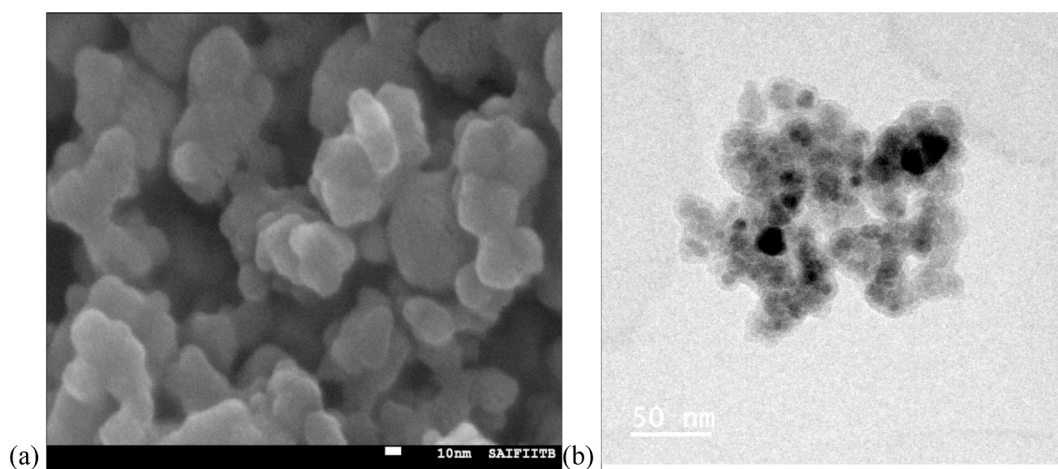


Fig. 1. The representative FESEM (a) and HRTEM images of the gel-like Fe_3O_4 -PEI (b).

reaction conditions, and results are summarized in [Table 1](#).

The reaction shown in [Scheme 4](#) did not proceed and did not yield any product without any catalyst for an observation period of 24 h. In the next step, this reaction was performed in the presence of various Fe_3O_4 -Imine catalysts shown in [Scheme 1](#) in different solvents at room

temperature. As can be seen from [Table 1](#), the Fe_3O_4 -Imine-Cu(II) catalyst having imine functional group **1a** yielded 94% of product when the reaction was conducted in water for 24 h (entry 1, [Table 1](#)). To understand the solvent effect, the reaction was also performed in protic solvents such as MeOH, EtOH, but only ~40% of product was formed

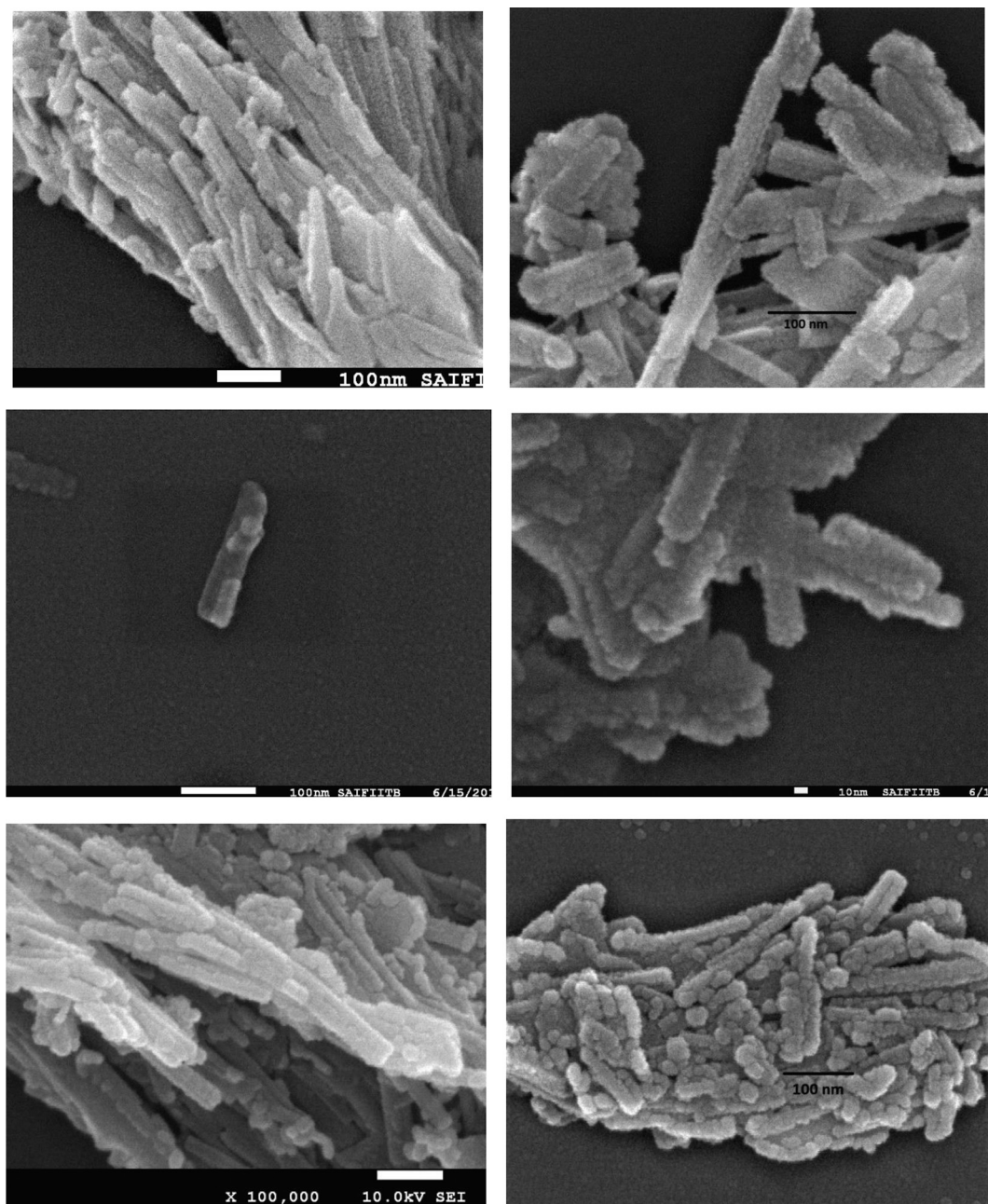


Fig. 2. The representative FESEM images of Fe_3O_4 -Imine showing the formation of the corn-like polymer nanoassemblies having varying lengths.

(entries 2 & 3, Table 1). This model reaction in the mixture of solvents (MeOH-H₂O (1:1)) afforded 60% of product formation (entry 4, Table 1). Polar aprotic solvents such as DMF did not improve the yield to a significant extent (entry 5, Table 1). The catalytic activities of Fe_3O_4 -Imine-Cu(II) catalysts loaded with various copper salts such as Cu(OAc)₂, CuBr₂, CuCl₂ were also studied. Among these, the Fe_3O_4 -Imine-Cu(II) catalyst loaded with Cu(OAc)₂ showed better results than those loaded with other copper salts. HPLC analysis of the nitroaldol adduct revealed that it was a racemic mixture having 49:51 proportion when Fe_3O_4 -Imine-Cu(OAc)₂ catalyst having functional group 1a was used.

To make an enantiomerically pure product, the Fe_3O_4 -Imine-Cu(II) catalysts (2a), (3a), (4a), (5a) and (6a) formed by using various chiral aldehyde were studied. The HPLC analyses of the resultant product did not show any enantiomeric excess with any of these catalysts used and yields of the product also remained the same. This seemed to suggest that the imine functional groups formed by using different chiral

aldehyde did not possess enough rigidity required for forming the enantiomerically pure product. This may be due to the motion of the hydrated polymer backbone which may offer random catalytic sites of the Cu(II)-amine catalyst to the reactants. Since catalyst (1a) showed better result in terms of yield, this catalyst under the optimized reaction conditions with water as the solvent was subjected to further studies. The reusability of the catalyst Fe_3O_4 -Imine-Cu(II) was checked for six successive cycling after washing, and no significant decrease in the catalytic activity in the model reaction shown in Scheme 4 was observed, see Fig. 4.

After optimizing the reaction conditions, the catalytic activity of Fe_3O_4 -Imine-Cu(OAc)₂ was studied for a variety of aldehyde derivatives reactants for the Henry reactions and results are shown in Table 2. Among the aromatic unsubstituted aldehydes, benzaldehyde gave the best yield (entry 3, Table 2). Similarly, among halogen derivatives (entry 4, and 6, Table 2), the bromo-derivative gave better yield. 2-

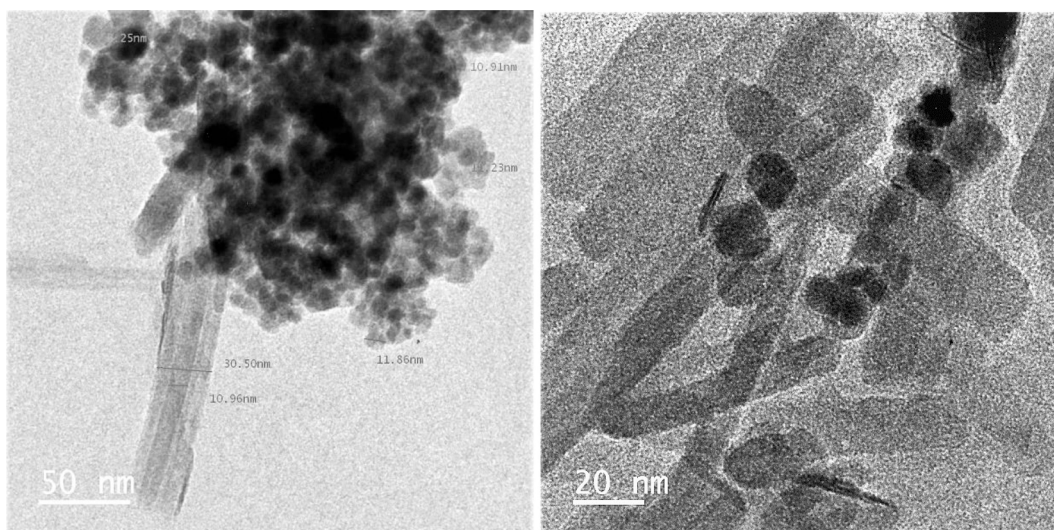
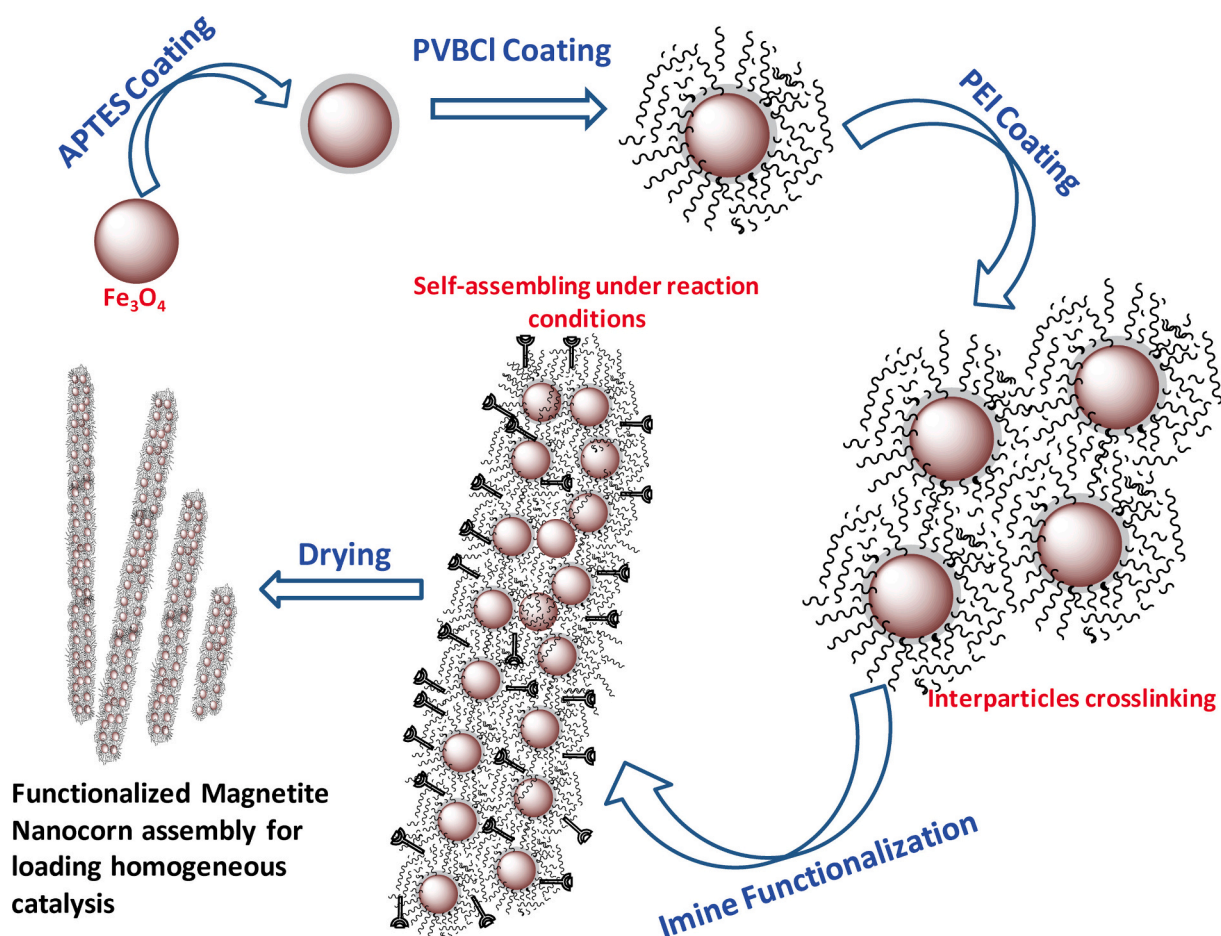


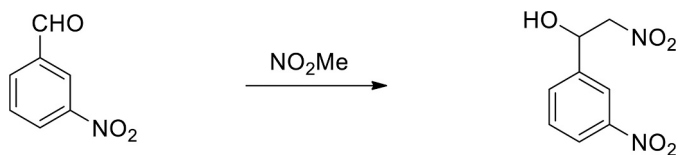
Fig. 3. The representative HRTEM images of the Fe_3O_4 -Imine corn-like nanoassemblies.



Scheme 3. Representation of morphological changes during different steps involved in the formation of corn-shaped Fe_3O_4 -Imine polymer nanoassemblies having varying lengths.

Nitrobenzaldehyde gave better yield (96% yield) than with meta-derivative probably due to the activation of aldehyde through secondary interaction of NO_2 group with CHO group (entry 1–2, Table 2). Reaction with aldehyde having preinstalled electron releasing substituent (entry 5, Table 2) furnished the corresponding product in a good yield. Reaction was found to be successful with even aliphatic aldehyde

(entry 8, Table 2) to afford corresponding adduct 60% yield. Reaction of pyridine 3-carbaldehyde, 4-cyano benzaldehyde and aldehyde with multiple substituents afforded nitroaldol product in a reasonably good (entry 7 and 9, Table 2).



Scheme 4. Model Henry reaction studied for the optimization of the reaction conditions at room temperature.

Table 1

Optimization and standardization of the reaction conditions for a model reaction shown in [Scheme 4](#) using different Cu(II) loaded Fe₃O₄-imine catalysts shown in [Schemes 1 & 2](#).

Entry no.	Catalyst (structure)	Solvent	Time (h)	Yield (%)
1	Fe ₃ O ₄ -Imine-Cu(OAc) ₂ (1a)	water	24	94
2	Fe ₃ O ₄ -Imine-Cu(OAc) ₂ (1a)	Methanol	36	40
3	Fe ₃ O ₄ -Imine-Cu(OAc) ₂ (1a)	Ethanol	36	39
4	Fe ₃ O ₄ -Imine-Cu(OAc) ₂ (1a)	Water: Methanol	48	60
5	Fe ₃ O ₄ -Imine-Cu(OAc) ₂ (1a)	DMF	48	20
6	Fe ₃ O ₄ -Imine-CuBr ₂ (1a)	water	24	81
7	Fe ₃ O ₄ -Imine-CuCl ₂ (1a)	water	24	83
8	Fe ₃ O ₄ -Imine-Cu(OAc) ₂ (2a)	water	24	70
9	Fe ₃ O ₄ -Imine-Cu(OAc) ₂ (3a)	water	24	79
10	Fe ₃ O ₄ -Imine-Cu(OAc) ₂ (4a)	water	24	72
11	Fe ₃ O ₄ -Imine-Cu(OAc) ₂ (5a)	water	24	76
12	Fe ₃ O ₄ -Imine-Cu(OAc) ₂ (6a)	water	24	68

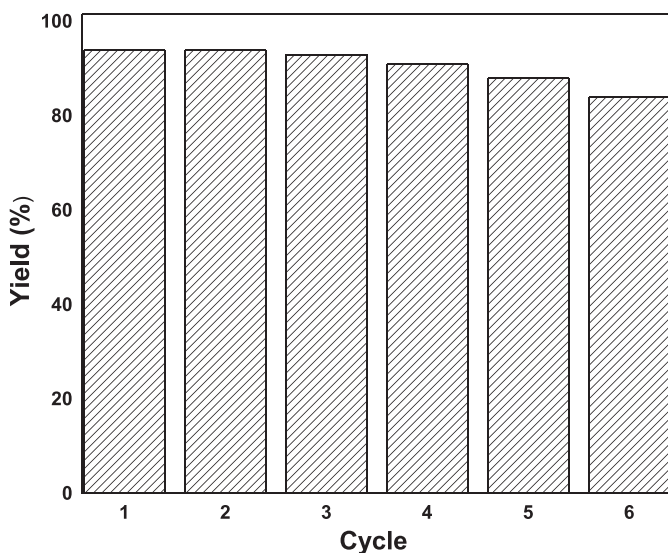


Fig. 4. The reusability Fe₃O₄-Imine-Cu(II) in model Henry reactions given in [Scheme 4](#). The reaction was carried out with 10 mg of the catalyst (Cu loading: 2.35×10^{-4} mol/g) and 5 mL water at RT.

3.5. A³-coupling reactions

The catalyst Fe₃O₄-Imine-Cu(OAc)₂ (1a) was studied for catalyzing the A³-coupling reaction of the type shown in [Scheme 5](#).

The chemical conditions for the model reaction shown in [Scheme 5](#)

were optimized for the catalyst Fe₃O₄-Imine-Cu(OAc)₂ (1a). As shown in Table S3 (Appendix A), this model multicoupling reaction did not proceed in the absence of catalyst, or in the presence of intermediates materials shown in [Scheme 1](#), or in the presence Fe₃O₄-Imine-Cu(OAc)₂ with water/methanol. But in the absence of the solvent, this reaction proceeded well with ≈60% yield in the presence of Fe₃O₄-Imine-Cu(OAc)₂ irrespective of its functional groups formed by using different aldehydes shown in [Scheme 2](#). Thus optimized reaction conditions were extended to the A³-coupling reactions involving aldehyde, pyrrolidine and phenyl acetylene having different substituents. As can be seen from [Table 3](#), the A³-coupling reactions afforded a reasonable good yield in 6 h except for entry no. 4 in [Table 3](#) which proceeded with a slightly lower rate. The TON and TOF numbers for the model reaction showed shown in [Scheme 5](#) were found to be reasonably good as 287 and 47.8 h⁻¹, respectively.

3.6. Comparison with other catalysts

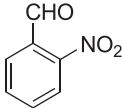
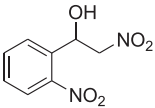
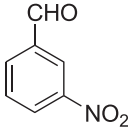
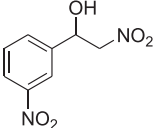
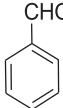
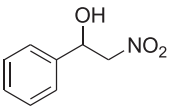
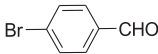
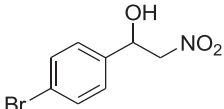
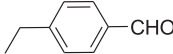
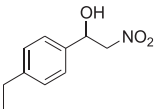
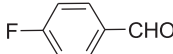
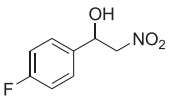
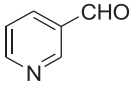
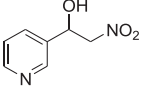
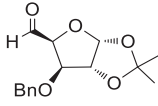
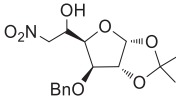
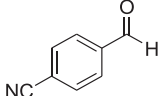
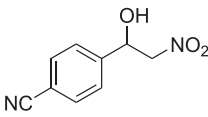
The catalytic efficiency of Fe₃O₄-Imine-Cu(OAc)₂ was compared with its precursor Fe₃O₄-PEI-Cu(OAc)₂ and other catalysts reported in the literature for the model Henry reaction and multicoupling A³-coupling reactions shown in [Schemes 4 and 5](#), respectively. The multicoupling reaction was first time studied and, therefore, no literature was available. It is evident from the data given in [Table 4](#) that the catalyst with imine functionalization improved the yield of model Henry reaction with respect to its precursor PEI. This could be attributed to higher water content in Fe₃O₄-Imine-Cu(OAc)₂ with respect to Fe₃O₄-PEI-Cu(OAc)₂ which would make Fe₃O₄-Imine-Cu(OAc)₂ more compatible with the aqueous medium containing reactants. This resulted in the increase of yield to 94% with Fe₃O₄-Imine-Cu(OAc)₂ as compared to 65% in the presence of Fe₃O₄-PEI-Cu(OAc)₂. However, this trend was reversed when ethanol was used to conduct the Henry reaction i.e. Fe₃O₄-PEI-Cu(OAc)₂ gave better yield (80%) with respect to Fe₃O₄-Imine-Cu(OAc)₂ (39%) under similar conditions. This suggested that the Fe₃O₄-PEI-Cu(OAc)₂ was more compatible with an ethanol solution containing reactants. It is seen from [Table 4](#) that the Fe₃O₄-Imine-Cu(OAc)₂ exhibited comparable catalytic efficiency in the Henry reaction with that reported in the literature using a homogeneous catalyst such as DNA in water at 12 °C [36]. However, the TOF and TON numbers were not reported in the literature, and hence quantitative comparison could not be done. Similar to Henry reaction, the catalytic efficiency of Fe₃O₄-Imine-Cu(OAc)₂ in the A³-coupling reactions without any solvent was considerably better as compared to that obtained by using Fe₃O₄-PEI-Cu(OAc)₂ under similar conditions as shown in [Table 4](#).

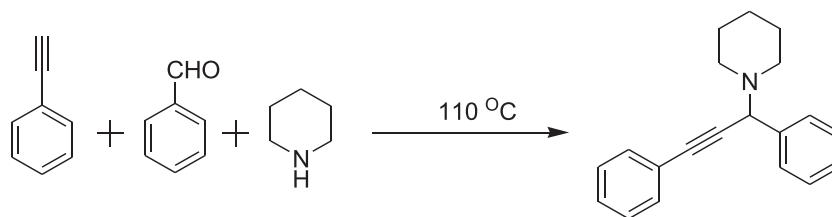
4. Conclusions

The imine-functionalized corn-like polymer nanoassemblies were formed for loading the copper salts, which are generally used as homogeneous catalysts in the organic reactions. The corn-like polymer nanoassemblies were formed due to stacking of the coated magnetite particles held together by the crosslinking of overlapping polymer shells. The formation of desired chemical structures on the magnetite NPs were confirmed by the FTIR studies and CHNS analyses. It was observed that ≈1.2 wt% of Cu(II) could be loaded on the Fe₃O₄-Imine nanoassemblies irrespective of their chemical structures. Among Cu(OAc)₂, CuBr₂, CuCl₂ salts, the Cu(OAc)₂ loaded Fe₃O₄-Imine nanoassemblies exhibited maximum catalytic activity in a model Henry reaction involving reaction of 3-nitrobenzaldehyde with nitromethane in the water at room temperature. The catalyst developed in the present work was also found to be successful in catalyzing the selected examples of multicoupling A³-coupling reactions of aldehyde, pyrrolidine, and phenyl acetylene at 110 °C temperature without the use of any solvent. The TON and TOF numbers for the model A³-coupling reactions were found to be reasonably good as 287 and 47.8 h⁻¹, respectively. The catalyst with imine functionalization (Fe₃O₄-Imine-Cu(OAc)₂) improved the

Table 2

The variations of yields in the Henry reactions were studied in the presence of 10 mg Fe_3O_4 -Imine- $\text{Cu}(\text{OAc})_2$ (1a) catalyst and 1 mmol of aldehyde, 10 mmol of nitromethane in 1 mL of water at room temperature.

Entry No.	Aldehyde	Product	Time (h)	Yield (%)
1			22	96
2			28	90
3			26	98
4			36	93
5			25	81
6			22	89
7			28	76
8			24	70
9			26	97



Scheme 5. Model A³-coupling reaction studied for the optimization of reaction conditions.

Table 3

The product yields obtained in the A³-coupling reactions studied in the presence of 10 mg Fe₃O₄-Imine-Cu(OAc)₂ catalyst (**1a**) and 1 mmol of aldehyde, 1 mmol of pyrrolidine, and 1 mmol of phenyl acetylene at 110 °C temp.

Entry No.	Aldehyde	Amine	Acetylene	Product	Time (h)	Yield (%)
1					6	67
2					6	63
3					6	65
4					7	59

Table 4

Comparison of catalytic activity of Fe₃O₄-Imine-Cu(OAc)₂ with other catalysts for the Henry reaction and Multicomponent couplings reaction given in Schemes 4 and 5, respectively.

Reaction	Catalyst	Solvent	Temp.	Time (h)	Yield (%)	Ref.
Henry reaction (Scheme 4)	Fe ₃ O ₄ -Imine-Cu(OAc) ₂	Water	R.T.	24	94	Present work
	Fe ₃ O ₄ -Imine-Cu(OAc) ₂	Ethanol	R.T.	36	39	Present work
	Fe ₃ O ₄ -PEI-Cu(OAc) ₂	Water	R.T.	28	65	[50]
	Fe ₃ O ₄ -PEI-Cu(OAc) ₂	Ethanol	R.T.	24	80	[50]
	DNA	Water	12 °C	8	90	[36]
	D-aminoacylase	DMSO	50 °C	0.5	80	[52]
Multicomponent reaction (Scheme 5)	Fe ₃ O ₄ -Imine-Cu(OAc) ₂	No solvent	110 °C	6	67	Present work
	Fe ₃ O ₄ -PEI-Cu(OAc) ₂	No solvent	110 °C	28	55	Present work

yield of model Henry reaction considerably with respect to its precursor PEI ($\text{Fe}_3\text{O}_4\text{-PEI-Cu(OAc)}_2$). This could be attributed to higher water content in $\text{Fe}_3\text{O}_4\text{-Imine-Cu(OAc)}_2$ with respect to $\text{Fe}_3\text{O}_4\text{-PEI-Cu(OAc)}_2$ which would make $\text{Fe}_3\text{O}_4\text{-Imine-Cu(OAc)}_2$ more compatible with the aqueous medium containing reactants. For A^3 -coupling reactions also, the kinetics and yield were found to be better by using the catalyst $\text{Fe}_3\text{O}_4\text{-Imine-Cu(OAc)}_2$ than that obtained by using $\text{Fe}_3\text{O}_4\text{-PEI-Cu(OAc)}_2$. Thus, the present work demonstrates the possibilities of developing the magnetic polymer nanoplatform having an appropriate functional group for loading the variety of metal salts generally used as the homogeneous catalysts in the various organic transformations in water. The polymer base provides the sites for anchoring the desired homogeneous catalyst, and superparamagnetic properties makes retrieval of these particles easier from the reaction solvent for the recycling without affected their catalytic efficacy.

Declaration of Competing Interest

None.

Acknowledgment

Authors are thankful to SAIF, IIT Bombay, Mumbai for FESEM and CHN analyses, and Physics Department, University of Savitribai Phule Pune University, Pune for VSM analyses. PBR thanks the Board of Research in Nuclear Science (BRNS), DAE, India for the financial assistance under BARC-University of Pune MoU for the Doctoral studies.

Appendix A. Supplementary data

Supplementary data to this article can be found online at <https://doi.org/10.1016/j.reactfunctpolym.2021.104868>.

References

- [1] D. Jagadeesan, Multifunctional nanocatalysts for tandem reactions: a leap toward sustainability, *Appl. Catal. A* 511 (2016) 59–77.
- [2] P. Munnik, P.E. de Jongh, K.P. de Jong, Recent developments in the synthesis of supported catalysts, *Chem. Rev.* 115 (2015) 6687–6718.
- [3] Y. Zhang, P. Liu, B.-G. Li, W.-J. Wang, CO_2 -triggered recoverable metal catalyst nanoreactors using unimolecular core-shell star copolymers as carriers, *ACS Appl. Nano Mater.* 1 (2018) 1280–1290.
- [4] W. Gan, H. Xu, X. Jin, X. Cao, H. Gao, Recyclable palladium-loaded hyperbranched polytriazoles as efficient polymer catalysts for Heck reaction, *ACS Appl. Polym. Mater.* 2 (2020) 677–684.
- [5] T. Verheyen, N. Santillo, D. Marinelli, E. Petricci, W.M. De Borggraeve, L. Vaccaro, M. Smet, An effective and reusable hyperbranched polymer immobilized rhodium catalyst for the hydroformylation of olefins, *ACS Appl. Polym. Mater.* 1 (2019) 1496–1504.
- [6] S. Chappa, P.B. Rathod, A.K. Debnath, D. Sen, A.K. Pandey, Palladium nanoparticles hosted in poly(ethylenimine) and poly(ethylene glycol methacrylate phosphate) anchored membranes for catalyzing uranyl ions reduction and Mizoroki-Heck coupling reaction, *ACS Appl. Nano Mater.* 1 (2018) 3259–3268.
- [7] L.M. Rossi, N.J.S. Costa, F.P. Silva, R.V. Gonçalves, Magnetic nanocatalysts: supported metal nanoparticles for catalytic applications, *Nanotechnol. Rev.* 2 (2013) 597–614.
- [8] L.M. Rossi, N.J.S. Costa, F.P. Silva, R. Wojcieszak, Magnetic nanomaterials in catalysis: advanced catalysts for magnetic separation and beyond, *Green Chem.* 16 (2014) 2906–2933.
- [9] R. Hudson, Y. Feng, R.S. Varma, A. Moores, Bare magnetic nanoparticles: sustainable synthesis and applications in catalytic organic transformations, *Green Chem.* 16 (2014) 4493–4505.
- [10] M.B. Gawande, P.S. Branco, R.S. Varma, Nano-magnetite (Fe_3O_4) as a support for recyclable catalysts in the development of sustainable methodologies, *Chem. Soc. Rev.* 42 (2013) 3371–3393.
- [11] R.K. Sharma, S. Dutta, S. Sharma, R. Zboril, R.S. Varma, M.B. Gawande, Fe_3O_4 (iron oxide)-supported nanocatalysts: synthesis, characterization and applications in coupling reactions, *Green Chem.* 18 (2016) 3184–3209.
- [12] A. Baeza, G. Guillena, D.J. Ramon, Magnetite and metal-impregnated magnetite catalysts in organic synthesis: a very old concept with new promising perspectives, *ChemCatChem* 8 (2016) 49–67.
- [13] R. Martinez, D.J. Ramon, M. Yus, Unmodified nano-powder magnetite catalyzes a four-component Aza-Sakurai reaction, *Adv. Synth. Catal.* 350 (2008) 1235–1240.
- [14] T. Ramani, P. Umadevi, K.L. Prasanth, B. Sreedhar, Synthesis of ortho-hydroxybenzophenones catalyzed by magnetically retrievable Fe_3O_4 nanoparticles under ligand-free conditions, *Eur. J. Org. Chem.* (2013) 6021–6026.
- [15] R. Dalpozzo, Magnetic nanoparticle supports for asymmetric catalysts, *Green Chem.* 17 (2015) 3671–3686.
- [16] R.B.N. Baig, R.S. Varma, Magnetically retrievable catalysts for organic synthesis, *Chem. Commun.* 49 (2013) 752–770.
- [17] P.B. Rathod, K.S. Ajish Kumar, A.A. Athawale, A.K. Pandey, S. Chattopadhyay, Polymer-shell-encapsulated magnetite nanoparticles bearing hexamethylenetetramine for catalyzing aza-Michael addition reactions, *Eur. J. Org. Chem.* (2018) 5980–5987.
- [18] P.B. Rathod, K.S. Ajish Kumar, S. Chappa, A.K. Debnath, A.K. Pandey, A. Athawale, Pd^{2+} -loaded magnetic nanoassembly formed by magnetite nanoparticles crosslinked with poly(acrylic acid) via amide bonds for catalyzing Mizoroki-Heck coupling reaction, *Chem. Select* 3 (2018) 8151–8158.
- [19] T. Cheng, D. Zhang, H. Li, G. Liu, Magnetically recoverable nanoparticles as efficient catalysts for organic transformations in aqueous medium, *Green Chem.* 16 (2014) 3401–3427.
- [20] Y. Zhu, L.P. Stubbs, F. Ho, R. Liu, C.P. Ship, J.A. Maguire, N.S. Hosmane, Magnetic nanocomposites: a new perspective in catalysis, *ChemCatChem* 2 (2010) 365–374.
- [21] V. Campisciano, A.M.P. Salvo, L.F. Liotta, A. Spinella, F. Giacalone, M. Gruttadauria, Cross-linked polyamine from imidazolium-based materials: a simple route to useful catalytic materials, *Eur. J. Org. Chem.* (2018) 1352–1358.
- [22] H. Veisi, S. Hemmati, P. Safarimehr, In situ immobilized palladium nanoparticles on surface of polymethylidopa coated-magnetic nanoparticles ($\text{Fe}_3\text{O}_4\text{-PMDA/Pd}$): a magnetically recyclable nanocatalyst for cyanation of aryl halides with $\text{K}_4[\text{Fe}(\text{CN})_6]$, *J. Catal.* 365 (2018) 204–212.
- [23] I. Misztalewska-Turkiewicz, K.H. Markiewicz, M. Michalak, A.Z. Wilczewska, NHC-copper complexes immobilized on magnetic nanoparticles: synthesis and catalytic activity in the CuAAC reactions, *J. Catal.* 362 (2018) 46–54.
- [24] A.J. Chancellor, B.T. Seymour, B. Zhao, Characterizing polymer-grafted nanoparticles: from basic defining parameters to behavior in solvents and self-assembled structures, *Anal. Chem.* 91 (2019) 6391–6402.
- [25] Y.-H. Xue, Y.-L. Zhu, W. Quan, F.-H. Qu, C. Han, J.-T. Fan, H. Liu, Polymer-grafted nanoparticles prepared by surface-initiated polymerization: the characterization of polymer chain conformation, grafting density and polydispersity correlated to the grafting surface curvature, *Phys. Chem. Chem. Phys.* 15 (2013) 15356–15364.
- [26] Z. Mokadem, S. Saidi-Besbes, N. Lebaz, A. Elaissari, Magnetic monolithic polymers prepared from high internal phase emulsions and Fe_3O_4 triazole-functionalized nanoparticles for Pb^{2+} , Cu^{2+} and Zn^{2+} removal, *React. Funct. Polym.* 155 (2020), 104693.
- [27] S.R. Chemler, Copper catalysis in organic synthesis, *Beilstein, J. Org. Chem.* 11 (2015) 2252–2253.
- [28] S. Thapa, B. Shrestha, S.K. Gurung, R. Giri, Copper-catalyzed cross-coupling: an untapped potential, *Org. Biomol. Chem.* 13 (2015) 4816–4827.
- [29] X.-X. Guo, D.-W. Gu, Z. Wu, W. Zhang, Copper-catalyzed C–H functionalization reactions: efficient synthesis of heterocycles, *Chem. Rev.* 115 (2015) 1622–1651.
- [30] R.-P. Ye, L. Lin, Q. Li, Z. Zhou, T. Wang, C.K. Russell, H. Adidharma, Z. Xu, Y.-G. Yao, M. Fan, Recent progress in improving the stability of copper-based catalysts for hydrogenation of carbon-oxygen bonds, *Catal. Sci. Technol.* 8 (2018) 3428–3449.
- [31] A.M. Thomas, A. Sujatha, G. Anil kumar, recent advances and perspectives in copper catalyzed Sonogashira coupling reactions, *RSC Adv.* 4 (2014) 21688–21698.
- [32] C.-y. Chen, F. He, G. Tang, H. Ding, Z. Wang, D. Li, L. Deng, R. Faessler, A copper-catalyzed tandem C–H ortho-hydroxylation and N–N bond-formation transformation: expedited synthesis of 1-(ortho-hydroxyaryl)-1h-indazoles, *Eur. J. Org. Chem.* (2017) 6604–6608.
- [33] A.V. Davis, M. Driffield, D.K. Smith, A dendritic active site: catalysis of the Henry reaction, *Org. Lett.* 3 (2001) 3075–3078.
- [34] M. Phukan, K.J. Borah, R. Borah, Henry reaction in environmentally benign methods using imidazole as a catalyst, *Green Chem. Lett. Rev.* 2 (2009) 249–253.
- [35] S.E. Milner, T.S. Moody, A.R. Maguire, Biocatalytic approaches to the Henry (Nitroaldol) reaction, *Eur. J. Org. Chem.* 16 (2012) 3059–3067.
- [36] J. Fan, G. Sun, C. Wan, Z. Wang, Y. Li, Investigation of DNA as a catalyst for Henry reaction in water, *Chem. Commun.* (2008) 3792–3794.
- [37] A.V. Gurbanov, S. Hazra, A.M. Maharramov, F.I. Zubkov, F.I. Guseinov, A.J. L. Pombeiro, The Henry reaction catalyzed by Ni^{II} and Cu^{II} complexes bearing arylhydrazones of acetoacetanilide, *J. Organometal. Chem.* 869 (2018) 48–53.
- [38] F.A. Luzzio, The Henry reaction: recent examples, *Tetrahedron* 57 (2001) 915–945.
- [39] R. Ballini, G. Bosica, D. Livi, A. Palmeiri, R. Maggi, G. Sartori, Use of heterogeneous catalyst KG-60-NET2 in Michael and Henry reactions involving nitroalkanes, *Tetrahedron Lett.* 44 (2003) 2271–2273.
- [40] A. Cwik, A. Fuchs, Z. Hell, J.-M. Clacens, Nitroaldol-reaction of aldehydes in the presence of non-activated Mg:Al 2:1 hydrotalcite; a possible new mechanism for the formation of 2-aryl-1,3-dinitropropanes, *Tetrahedron* 61 (2005) 4015–4021.
- [41] J.A. Weeden, J.D. Chisholm, Phosphine-catalyzed nitroaldol reactions, *Tetrahedron Lett.* 47 (2006) 9313–9316.
- [42] M. Solinas, B. Sechi, S. Baldino, G. Chelucci, Synthesis and application of new iminopyridine ligands to enantioselective copper(II)-catalyzed Henry reaction, *J. Mol. Catal. A Chem.* 378 (2013) 206–212.
- [43] G. Lu, F. Zheng, L. Wang, Y. Guo, X. Li, X. Cao, C. Wang, H. Chi, Y. Dong, Z. Zhang, Asymmetric Henry reaction catalyzed by $\text{Cu}(\text{II})$ -based chiral amino alcohol complexes with C2-symmetry, *Tetrahedron* 27 (2016) 732–739.

- [44] Q. Song, X. An, T. Xia, X. Zhou, T. Shen, Catalytic asymmetric Henry reaction using copper(II) chiral tridentate Schiff-base complexes and their polymer-supported complexes, *Comp. Rendus Chim.* 18 (2015) 215–222.
- [45] T. Arai, M. Watanabe, A. Yanagisawa, Practical asymmetric Henry reaction catalyzed by a chiral diamine-Cu(OAc)₂ complex, *Org. Lett.* 9 (2007) 3595–3597.
- [46] A. Karmakar, S. Hazra, M.F.C. Guedes da Silva, A.J.L. Pombeiro, Synthesis, structure and catalytic applications of amidoterephthalate copper complexes in the diastereoselective Henry reaction in aqueous medium, *New J. Chem.* 38 (2014) 4837–4846.
- [47] D.S. Bhosale, P. Drabina, M. Kincl, M. Vlček, M. Sedlák, Magnetically recoverable catalyst for the asymmetric Henry reaction based on a substituted imidazolidine-4-one copper(II) complex supported by Fe₃O₄-SiO₂ nanoparticles, *Tetrahedron* 26 (2015) 1300–1306.
- [48] A.V. Biradar, K.K. Sharma, T. Asefa, Continuous Henry reaction to a specific product over nanoporous silica-supported amine catalysts on fixed bed reactor, *Appl. Catal. A* 389 (2010) 19–26.
- [49] F. Rafiee, F.R. Karder, Synthesis and characterization of magnetic glycoamine-modified chitosan as a biosupport for the copper immobilization and its catalytic activity investigation, *React. Funct. Polym.* 146 (2020) 104434.
- [50] P.B. Rathod, S. Chappa, K.S. Ajish Kumar, A.K. Pandey, A.A. Athawale, Poly(ethylenimine) functionalized magnetic nanoparticles for sorption of Pb, Cu, and Ni: potential application in catalysis, *Sep. Sci. Technol.* 54 (2019) 1588–1598.
- [51] A. Movahedi, A. Lundin, N. Kann, M. Nydén, K. Moth-Poulsen, Cu(I) stabilizing crosslinked polyethyleneimine, *Phys. Chem. Chem. Phys.* 17 (2015) 18327–18336.
- [52] F. Xu, J. Wang, B. Liu, Q. Wu, X. Lin, Enzymatic synthesis of optical pure β-nitroalcohols by combining d-aminoacylase-catalyzed nitroaldol reaction and immobilized lipase PS-catalyzed kinetic resolution, *Green Chem.* 13 (2011) 2359–2361.